DBpia

논문 17-42-07-06 The Journal of Korean Institute of Communications and Information Sciences '17-07 Vol.42 No.07
https://doi.org/10.7840/kics.2017.42.7.1340

사용자간 상호상관의 첨도 분석 및 초광대역 거리추정에 미치는 영향

이 준 용◆°

Impulsiveness Analysis of Cross-Correlation between Users and Its Effect on the Ultra-Wideband Ranging

Joon-Yong Lee◆°

요 약

본 논문에서는 time hopping 및 direct sequence 방식의 초광대역 시스템에서, 사용자간 상호상관함수의 첨도를 분석하고 거리추정시스템의 성능에 미치는 영향을 평가한다. 사용자간 간섭특성의 분석을 위해 사용자간 상호상관함수의 분산을 측정하는 것이 일반적이다. 그러나 본 논문에서는 사용자간 상호상관함수의 첨도를 나타내는 파라미터인 kurtosis를 활용하였다. 정밀한 거리추정에 많이 사용되는 UWB 시스템의 특성상, 다중사용자 간섭신호의 첨도는 매우 중요한 특성이기 때문이다. 독립항등분포를 갖는 확산코드를 사용하였을 때, 두 다중접속 방식에서 분산값은 유사하게 나타났으나, kurtosis는 매우 다른 패턴을 보이는 것으로 나타났다. 수신단에서의 다중사용자 간섭을 평가하였을 때에도, 유사한 패턴이 얻어졌다. 항등분포코드 대신 유사잡음코드를 확산코드로 사용하였을 때에도 비슷한 결과가 얻어졌다. 다중접속자 방식에 따른 이러한 차이는 거리추정시 발생하는 오경보확률에 중대한 영향을 미치는 것으로 모의실험을 통해 확인되었다.

Key Words : Ultra-wideband, Ranging, Multiuser interference, Kurtosis analysis

ABSTRACT

In this paper, we evaluate the impulsiveness of the cross-correlation between the user signals for asynchronous time-hopping and direct-sequence ultra-wideband (UWB) transmissions and examine its effect on UWB ranging. It is conventional to measure variance of cross-correlation for interference analysis. However, kurtosis, a parameter indicating the impulsiveness, was utilized in this work. Considering the ranging applications of UWB systems, the impulsiveness of multiuser interference is critical. When an independent and identically distributed random spreading code was used, the variance for the two scenarios was shown to be similar but the kurtosis indicated a considerably different change pattern with respect to the sequence length. The evaluation of the multiuser interference term also exhibited similar results for both single-path and multipath scenarios. Similar results were obtained through simulations using pseudo noise sequence. A significant effect of the difference in impulsiveness on the probability of early false alarm error in a ranging scenario can be seen through simulations.

※ This research was supported in part by the Basic Science Research Program through the National Research Foundation of Korea (NRF) funded by the Ministry of Education, Science and Technology (NRF-2012R1A1A2041260) and in part by a Sabbatical Leave Grant at Handong Global University (HGU-2015).

◆° First and Corresponding Author : Handong University, School of Computer Science & Electrical Engineering, joonlee@handong.edu, 정회원

논문번호 : KICS2017-03-073, Received March 14, 2017; Revised June 4, 2017; Accepted June 15, 2017

www.dbpia.co.kr

Ⅰ. Introduction

There is a growing interest in indoor positioning systems and ultra-wideband (UWB) system has been considered as a viable solution[1-3]. UWB ranging applications involve not only multiple paths but also a large number of users [4]. In many UWB ranging systems, threshold detection is applied to the matched filter (MF) output at the receiving side. The system searches for a particular interval of MF output and chooses the first level-crossing point at the threshold as the time of arrival (ToA) of the direct path signal. If the MF output for the noise and interference-only portion of the signal is greater than the threshold, an early false alarm error occurs [5]. Fig. 1 illustrates this scenario. Thus, it is expected that the higher the impulsiveness of the multiuser interference (MUI) signal, the higher the probability of an early false alarm error. The impulsiveness of the MUI term can be measured by its kurtosis. The kurtosis of a random parameter Z is defined as

$$\mathrm{Kurt}[Z] = \frac{\mathrm{E}\left[(Z-m_z)^4\right]}{\sigma_z^4}, \qquad (1)$$

where m_z and σ_z denote the mean and standard deviation of Z, respectively. There has been controversy regarding the exact meaning of kurtosis. Currently, a widely accepted interpretation is that kurtosis is mostly determined by the tail shape of the probability density function [6]. According to [7], a large kurtosis indicates that the variance of the random parameter is the result of infrequent extreme deviations rather than frequent modestly sized deviations; i.e., for a similar variance, the larger the kurtosis value, the greater is the probability of occurrence of an extreme value. Therefore, the kurtosis of the MUI term at the receiver is closely related to its impulsiveness.

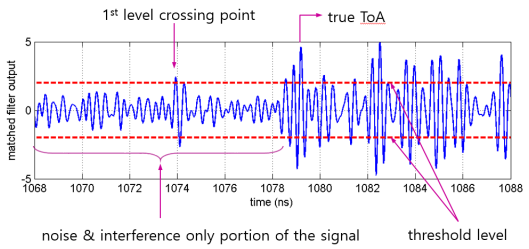

Fig. 1. UWB ToA estimation scenario. Noise and interference may cause an early false alarm error.

A good correlation property between users is an important criterion for the spreading code design [8-13] along with spectral flatness[5,6,11,12] and narrowband interference suppression[13,14]. Variance has been commonly used as a quality measure in the examination of the properties of cross-correlation, whereas the kurtosis has not been examined. To evaluate the kurtosis of the MUI term at the receiving side, the kurtoses of the cross-correlation between different user signals are first compared under two typical multiple access (MA) scenarios: time hopping (TH) and direct sequence (DS). Our concern is to know how the kurtosis of the cross-correlation is affected by the different MA schemes rather than by the spreading code type. Comparative analysis of kurtoses of interference terms in different MA schemes is a unique contribution of this work. Furthermore, it is a very interesting finding that the kurtoses of MUI terms are remarkably different in the TH and DS cases.

In this work, we assumed that independent and identically distributed (iid) random spreading codes are employed for both the cases, and we compare the variance and kurtosis of the cross-correlation between the users. The analysis results are described in Section Ⅱ. Based on these results, the kurtosis of the MUI term in the environment where several users are present is compared between two MA scenarios in Section Ⅲ. As an example of a multiuser environment, a simplified single-path environment was assumed and both analysis and simulation were conducted. In order to evaluate the kurtosis of the MUI term in a more realistic environment, simulations were also conducted for an indoor multipath environment, and these results are described in Section Ⅳ. In Section Ⅴ, we examine the effect of a difference in kurtosis under two MA scenarios on ranging performance. More specifically, a probability of early false alarm error, which is one of the kinds of ranging errors [5], is evaluated

www.dbpia.co.kr

through simulations in the multipath and multiuser environment.

Ⅱ. Kurtosis of the cross-correlation between two users

As the first step, we evaluate the normalized cross-correlation between the two user signals under two MA scenarios. The tedious calculations of the moments are relegated to Appendix 1.

2.1 TH-MA

First, the TH UWB signal of the k^{th} user, without considering the modulation, can be expressed as [18]

$$s^{(k)}(t)=\sum_{j=-\infty}^{\infty} w\left(t-jT_{\text{f}}-c_j^{(k)}T_{\text{c}}\right), \tag{2}$$

where $w(t)$ is one-pulse template waveform. The parameter T_{f} and T_{c} denote the frame time and the chip time, respectively, and satisfy $N_{\text{h}}T_{\text{c}}=T_{\text{f}}$. The sequence $\left\{c_j^{(k)}\right\}$ is the TH code of the k^{th} user, and it satisfies $0\le c_j^{(k)}\le N_{\text{h}}-1$. Without loss of generality, we assume that the receiver is interested in the signal transmitted by user 0. The signal $s^{(k)}(t)$ can be expressed as a sequence $\left\{s_n^{(k)}\right\}$ as follows [8]:

$$s^{(k)}(t)=\sum_{j=-\infty}^{\infty}\delta_{\text{K}}\left(n-jN_{\text{h}}-c_j^{(k)}\right), \tag{3}$$

where $\delta_{\text{K}}(\cdot)$ denotes the Kronecker delta function. The binary value of $s_n^{(k)}$ indicates the presence or absence of a pulse in the time slot $t\in\left[(n-1)T_{\text{c}},nT_{\text{c}}\right]$; a binary 1 indicates the presence of a pulse and a binary 0 indicates its absence. If the period of the TH code $\left\{c_j^{(k)}\right\}$ is L, then the period of the sequence $\left\{s_n^{(k)}\right\}$ is LN_{h}. the cross-correlation between user 0 and the user k is defined as [8]

$$R_{0k}(\rho)=\frac{1}{L}\sum_{n=0}^{LN_{\text{h}}-1}s_n^{(0)}s_{\left[n-\rho\right]_{LN_{\text{h}}}}^{(k)}, \tag{4}$$

where the notation $\left[x\right]_y$ denotes x modulo y. Equation (4) indicates a cross-correlation function with a chip synchronism but without a frame synchronism. Expressing ρ as $\tau N_{\text{h}}+\phi$, where $\phi\in\{0,1,2,\cdots,N_{\text{h}}-1\}$, then,

$$R_{0k}(\tau N_{\text{h}}+\phi)=\frac{1}{L}\sum_{n=0}^{LN_{\text{h}}-1}s_n^{(0)}s_{\left[n-\tau N_{\text{mathrm}}h-\phi\right]_{LN_{\text{h}}}}^{(k)}. \tag{5}$$

A non-zero ϕ accounts for the frame asynchronism. For $\phi=0$, the following is satisfied:

$$\begin{aligned}R_{0k}(\tau N_{\text{h}})&=\frac{1}{L}\sum_{n=0}^{LN_{\text{h}}-1}s_n^{(0)}s_{\left[n-\tau N_{\text{h}}\right]_{LN_{\text{h}}}}^{(k)}\\&=\frac{1}{L}\sum_{j=0}^{L-1}\delta_{\text{K}}\left(c_j^{(0)}-c_{\left[j-\tau\right]_L}^{(k)}\right).\end{aligned} \tag{6}$$

Thus, for $\phi=0$, the cross-correlation between the signals $\left\{s_n^{(0)}\right\}$ and $\left\{s_n^{(k)}\right\}$ is equal to the cross-correlation between TH codes $\left\{c_j^{(0)}\right\}$ and $\left\{c_j^{(k)}\right\}$.

Now, let us calculate the moments of $R_{0k}(\tau N_{\text{h}}+\phi)$. In this paper, it is assumed that an iid random sequence is used for the TH code. For $\phi=0$, the moments can be easily calculated. However, if ϕ is random, i.e., if frame asynchronism is assumed, the calculation becomes complicated. This is because if $\phi=0$, the existence of a coincidence of two sequences within a frame can affect their coincidence in the adjacent frame. Intuitively, it can be expected that a random ϕ will not significantly affect the moments of $R_{0k}(\tau N_{\text{h}}+\phi)$ because the shift pattern of the pulse position is random in the case of TH. In this section, the moments of the cross-correlation are first calculated assuming,

$$\text{E}\left[R_{0k}^q(\tau N_{\text{h}}+\phi)\right]=\text{E}\left[R_{0k}^q(\tau N)\right],\forall\,0\le\phi\le N_{\text{h}}-1, \tag{7}$$

where q is a positive integer. The calculated results are then compared with the simulation results obtained with a random ϕ. (In section Ⅱ-3, the two

www.dbpia.co.kr

results are shown to be matched.) In Appendix 1-A, the moments of $R_{0k}(\tau N_{\mathrm{h}})$ up to the 4^{th} order are calculated assuming (7).

2.2 DS-MA

An analysis similar to that in the previous section is performed for the DS signal. The DS UWB signal can be represented by [19]

$$s^{(k)}(t)=\sum_{j=-\infty}^{\infty} b_j^{(k)} w(t-jT_{\mathrm{f}}), \tag{8}$$

where $\{b_j^{(k)}\}$ is the direct sequence code and $b_j^{(k)}\in\{-1,1\}$. This signal can be expressed as a ternary sequence $\{s_n^{(k)}\}$, given by,

$$s_n^{(k)}=\sum_{j=-\infty}^{\infty} b_j^{(k)}\delta_{\mathrm{K}}(n-jN_{\mathrm{h}}). \tag{9}$$

Each value $s_n^{(k)}\in\{-1,0,1\}$ represents the presence or absence of a pulse in the time slot $t\in[(n-1)T_{\mathrm{c}}, nT_{\mathrm{c}}]$ and its polarity. Note that the quantization step of $s^{(k)}(t)$ is selected as T_{c}, i.e., the same as in the case of TH, rather than T_{f}; the aim is to define the cross-correlation for an asynchronous scenario as in the case of TH. The cross-correlation $R_{0k}(\rho)$ between user 0 and user k can be defined as in (4), and it further satisfies

$$R_{0k}(\rho)=R_{0k}(\tau N_{\mathrm{h}}+\phi)=\frac{1}{L}\sum_{j=0}^{L-1} b_j^{(0)} b_{\lfloor j-\tau\rfloor_L}^{(k)}\delta_{\mathrm{K}}(\phi). \tag{10}$$

As the pulse is transmitted periodically, the cross-correlation becomes zero for $\phi\neq 0$. In Appendix 1, the moments of $R_{0k}(\tau N_{\mathrm{h}}+\phi)$ up to the 4^{th} order are derived, assuming that the spreading code $\{b_j^{(k)}\}$ is an iid random sequence and the parameter ϕ is also equally likely.

2.3 Comparison

Fig. 2 plots the variance and kurtosis among the moments calculated in Appendix 1. The variance is inversely proportional to L, which is similar in both

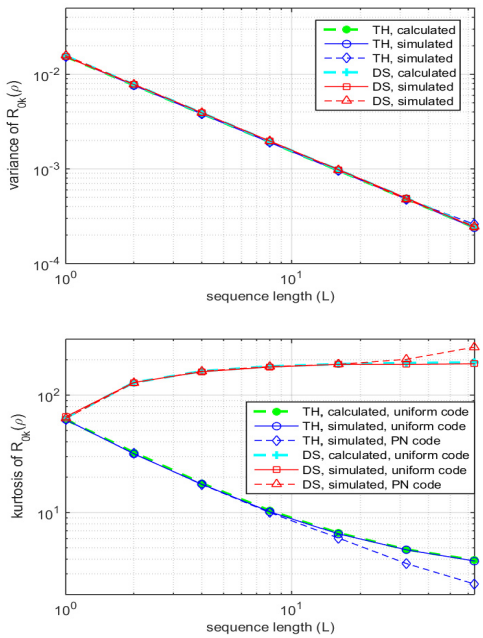

Fig. 2. Variance and kurtosis of the cross-correlation between the two users evaluated with $N_{\mathrm{h}}=64$. Simulation results obtained using PN codes are also shown.

the cases. For the kurtosis, the change in pattern according to L is remarkably different in the two scenarios. To examine the effect of the spreading codes employed in the system, we also carried out simulations using PN codes instead of uniform codes. For the TH system, a spreading sequence introduced by Scholtz et al. [8] was employed. This sequence is constructed using a finite field with an order of a prime number p; here, we select it to be 61. This provides 60 distinct time-hopping patterns of a period of 61. Out of 64 slots, 61 are chosen to be the possible hopping locations. A Gold sequence with a length of 63 was employed for the simulation of the DS case.

The quantity $R_{0k}(\rho)$ can be interpreted as the contribution of user k to the signal reception of user 0 averaged over L repeated pulse transmissions. Thus, as the number of integrations increases, it is natural that the variance of the interference term associated with user k decreases in both the cases. However, it is extremely interesting that the kurtosis, representing the impulsiveness, increases in the case of DS, whereas it decreases for TH. Not only in the

www.dbpia.co.kr

case of DS but also in the case of TH, the analytical values and the simulation results of the variance and kurtosis are well matched, indicating that the assumption given in (7) is valid. No substantial difference can be observed in the results obtained using uniform codes and PN codes.

The possible reason for the difference in the Kurtoses is that different UWB spread spectrum techniques employ different types of randomization: randomization of the shift pattern and/or polarity of the transmitting pulse. Accordingly, different averaging mechanisms are employed at the receiver, which affects the impulsiveness of MUI signal.

Ⅲ. Kurtosis of MUI term for a single-path scenario

In this section, the moment of the MUI term is evaluated assuming an environment where N_u+1 users are present, utilizing the results presented in section Ⅱ. As an example of a multiuser environment, we assume a single-path LoS environment wherein all the transmitters are distributed uniformly over a ring-shaped region between d_0 m and d m from the receiver (see Fig. 3). Then, the distance, r, between the transmitter and receiver is distributed as follows:

$$f_r(r)=\frac{2r}{d^2-d_0^2}. \tag{11}$$

The power, P_k, of the received signal from user k can be expressed as

$$P_k=a_k^2=\frac{G}{r^2}, \tag{12}$$

where G is a constant and a_k denotes the signal strength of the k^{th} user.

Let us define r_n as a collection of signals received from the other users, then,

$$r_n=\sum_{k=1}^{N_u}a_k s_{n-\rho_k}^{(k)},\ \rho_k=\tau_k N_h+\phi_k, \tag{13}$$

where $s_n^{(k)}$ is given by (3) and (9) for the TH and DS cases, respectively. If the MUI term I is defined as the cross-correlation between the sequences $\{s_n^{(0)}\}$ and $\{r_n\}$, then,

$$I=\sum_{k=1}^{N_u}a_k R_{0k}(\tau_k N_h+\phi_k). \tag{14}$$

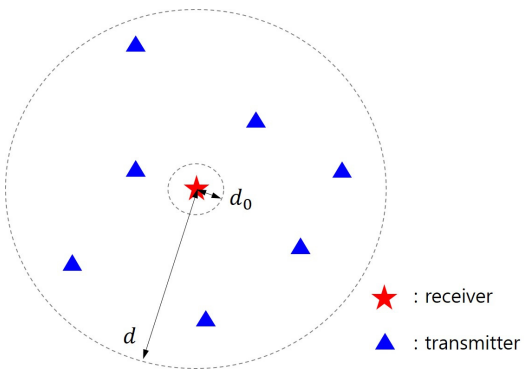

Fig. 3. Transmission scenario.

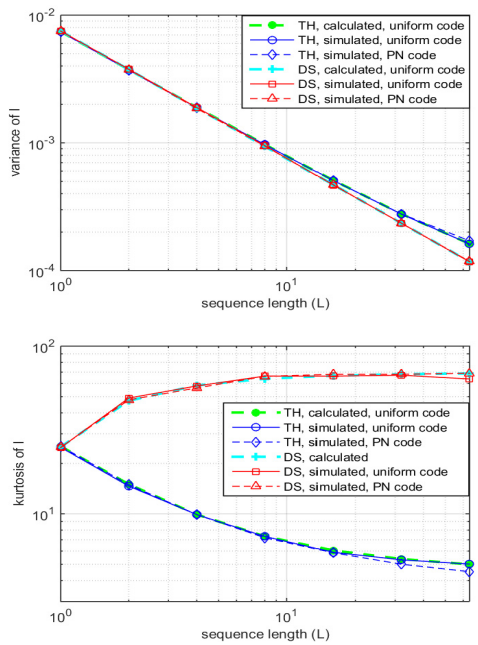

Fig. 4. Variance and kurtosis of I for a multiuser single-path environment evaluated with $N_h=64$, $N_u=32$, $G=1$ m, $d=20$ m, and $d_0=1$ m. Simulation results obtained using PN codes are also shown.

www.dbpia.co.kr

In Appendices 2-A and 2-B, the moments of I up to the 4^{th} order are calculated for the TH and DS cases, respectively. Fig. 4 plots the calculation and simulation results of the variance and kurtosis. In the figure, a pattern similar to that shown in Fig. 2 is observed. When the PN code is used for the DS case, the kurtosis is higher than in the case of uniform code with $N_{\text{h}} = 64$. This is probably because of the fact that the period of the Gold sequence (63) is less than the number of integrations.

Ⅳ. Kurtosis of MUI term for a multipath scenario

In this section, simulations are carried out for a more realistic multipath environment than that assumed in the previous section to evaluate the effect of the MA scheme on the impulsiveness of the MUI term. MUI signal $r(t)$ received through the multipath channel can be expressed as

$$r(t) = \sum_{k=1}^{N_{\text{u}}} h^{(k)}(t) * s^{(k)}(t - \psi_k), \tag{15}$$

where parameter ψ_k, which accounts for both frame asynchronism and chip asynchronism, is assumed to be uniform on $[0, T_{\text{f}}]$. Signal $s^{(k)}(t)$ is given by (2) and (8) for the TH and DS cases, respectively. The one-pulse template waveform $w(t)$ appearing in (2) and (8) is given by [20]

$$w(t) = A\exp(-at^2)\sin(\omega t), \tag{16}$$

where $a = 5.55$ and $\omega = 26.15$. Constant A is chosen to be 0.266 such that $w(t)$ has unit energy. The function $h^{(k)}(t)$ is the channel impulse response for the k^{th} user. In this study, IEEE 802.15.4a CM 3, which is a UWB channel model for an indoor LoS environment, was used for the simulation. The correlator template $v(t)$ at the receiving side is given by

$$v(t) = \sum_{j=0}^{L-1} w(t - jT_{\text{f}} - c_j^{(0)} T_{\text{c}}). \tag{17}$$

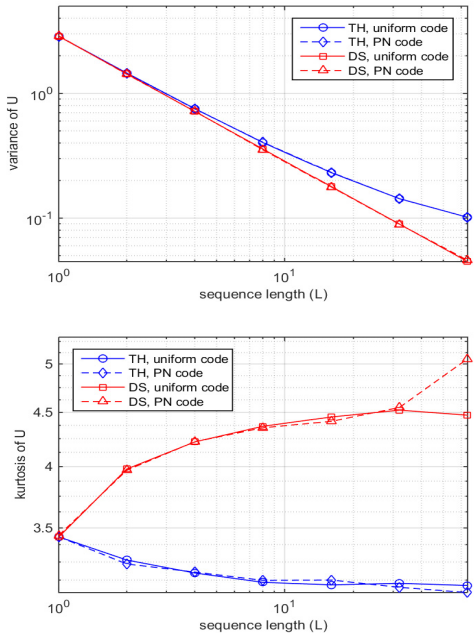

Fig. 5. Variance and kurtosis of U for a multiuser multipath environment simulated with $N_{\text{h}} = 64$, $N_{\text{u}} = 32$, and $T_{\text{c}} = 1$ ns. Simulation results obtained using PN codes are also shown.

Now, define the MUI term U as the normalized cross-correlation between $r(t)$ and $v(t)$, then,

$$U = \frac{1}{L}\int_0^{LT_{\text{f}}} r(t)v(t)dt. \tag{18}$$

Fig. 5 shows the simulation result for the kurtosis and variance of U. A similar pattern can be seen as in the results obtained in the previous sections.

Ⅴ. Ranging effect

In this section, the effect of the kurtosis of the MUI term, which has been evaluated in the previous section, on the ranging performance is evaluated through simulation. Here, it is assumed that the UWB ranging system employs threshold-based ToA estimation. In order to increase the signal-to-interference-plus-noise ratio of the signal, MF normally includes two-stage matching: a pulse waveform MF and a spreading sequence MF. As mentioned in section Ⅰ, if the MF output for the

www.dbpia.co.kr

noise and interference-only portion of the signal is greater than the threshold, the level-crossing point is falsely detected as the leading edge of the signal. Thus, the probability of an early false alarm error can be considered to be highly correlated with the impulsiveness of the MUI term.

To examine this effect, we first generated an MF output for the MUI signal of a specific length (frame time). Then, we carried out thresholding and observed whether a level-crossing occurred. The threshold θ was determined relative to the power of the generated signal, i.e.

$$\theta = \gamma \cdot \sigma_{\mathrm{m}}, \tag{19}$$

where γ is a constant and σ_{m} is the standard deviation of the matched filtered version of MUI signal. Fig. 6 shows the changes in early false alarm error probability according to L in the case of TH and DS. It is interesting that the result shown in this figure exhibits a pattern that is very similar to the result shown in Fig. 5. This result indicates that even if a threshold is selected as a constant multiple of the standard deviation of the MUI signal, the early false alarm error probability can be different due to the difference in the signal's kurtosis.

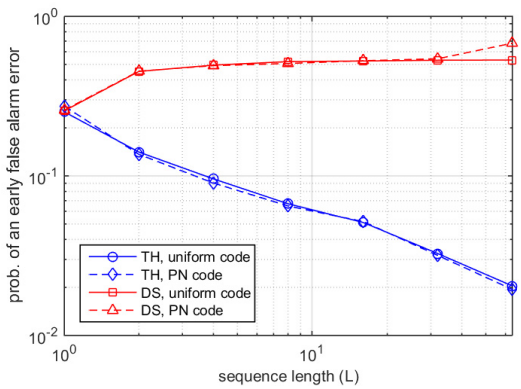

Fig. 6. Probability of an early false alarm error simulated with $N_{\mathrm{h}} = 64$, $N_{\mathrm{u}} = 32$, $T_{\mathrm{c}} = 1$ ns, and $\gamma = 4$. Simulation results obtained using PN codes are also shown.

Ⅵ. Conclusions

In this paper, the cross-correlation properties of TH and DS impulse radio signals were analyzed statistically and subsequently extended to a multiuser scenario. Comparison of the impulsiveness of the TH and DS UWB systems on the basis of the kurtosis of the MUI term is a unique contribution of this study. It is found that when employing spreading sequence matched filtering, the kurtoses of the MUI term are remarkably different for the two cases; this difference is assumed to be owing to the differences in the randomization methods of the TH and DS schemes. The simulation result showed that a difference in impulsiveness significantly affected the probability of an early false alarm error for time delay estimation in the multiuser multipath environment.

Appendix

1. Moments of cross-correlation between two users

A. TH-MA

Let us derive the moments of $R_{0k}(\tau N_{\mathrm{h}} + \phi)$ given in (5) for the TH case. Since we assumed (7), the moments of $R_{0k}(\tau N_{\mathrm{h}})$ are calculated in this section. First, the mean of $R_{0k}(\tau N_{\mathrm{h}})$ is given by

$$\mathrm{E}\left[R_{0k}(\tau N_{\mathrm{h}})\right] = \frac{1}{L}\sum_{j=0}^{L-1}\mathrm{E}\left[\delta_{\mathrm{K}}\left(c_j^{(0)} - c_{\lfloor j-\tau \rfloor_L}\right)\right]. \tag{20}$$

Since the delta function term in the above equation is a uniform random variable, it is obtained as

$$\mathrm{E}\left[R_{0k}(\tau N_{\mathrm{h}})\right] = \frac{1}{L}\sum_{j=0}^{L-1}\frac{1}{N_{\mathrm{h}}} = \frac{1}{N_{\mathrm{h}}}. \tag{21}$$

The 2^{nd} order moment is given by

$$\mathrm{E}\left[R_{0k}^2(\tau N_{\mathrm{h}})\right] = \frac{1}{L^2}\sum_{i=0}^{L-1}\sum_{j=0}^{L-1}\mathrm{E}\left[\delta_{\mathrm{K}}\left(c_i^{(0)} - c_{\lfloor i-\tau \rfloor_L}^{(k)}\right) \cdot \delta_{\mathrm{K}}\left(c_j^{(0)} - c_{\lfloor j-\tau \rfloor_L}^{(k)}\right)\right] \tag{22}$$

www.dbpia.co.kr

Here, breaking the sum into $i=j$ and $i\neq j$ parts, the above equation can be represented by

$$\mathrm{E}\left[R_{0k}^2(\tau N_\mathrm{h})\right]=\frac{1}{L^2}\sum_{i=0}^{L-1}\mathrm{E}\left[\delta_\mathrm{K}^2\left(c_i^{(0)}-c_{i+\tau}^{(k)}\right)\right]$$
$$+\frac{1}{L^2}\sum_{\substack{i=0\\ i\neq j}}^{L-1}\sum_{j=0}^{L-1}\mathrm{E}\left[\delta_\mathrm{K}\left(c_i^{(0)}-c_{i+\tau}^{(k)}\right)\delta_\mathrm{K}\left(c_j^{(0)}-c_{j+\tau}^{(k)}\right)\right]. \quad (23)$$

Taking advantage of independence,

$$\mathrm{E}\left[R_{0k}^2(\tau N_\mathrm{h})\right]=\frac{1}{L^2}\sum_{i=0}^{L-1}\frac{1}{N_\mathrm{h}}+\frac{1}{L^2}\sum_{\substack{i=0\\ i\neq j}}^{L-1}\sum_{j=0}^{L-1}\frac{1}{N_\mathrm{h}^2}$$
$$=\frac{N_\mathrm{h}+L-1}{LN_\mathrm{h}^2}. \quad (24)$$

Similarly, the 3^{rd} order moment is given by

$$\mathrm{E}\left[R_{0k}^3(\tau N_\mathrm{h})\right]=\frac{1}{L^3}\sum_{i=0}^{L-1}\sum_{j=0}^{L-1}\sum_{i'=0}^{L-1}\mathrm{E}\left[\delta_\mathrm{K}\left(c_i^{(0)}-c_{[i-\tau]_L}^{(k)}\right)\right.$$
$$\left.\cdot\,\delta_\mathrm{K}\left(c_j^{(0)}-c_{[j-\tau]_L}\right)\cdot\delta_\mathrm{K}\left(c_{i'}^{(0)}-c_{[i'-\tau]_L}^{(k)}\right)\right], \quad (25)$$

and breaking the sum into three parts, this reduces to

$$\mathrm{E}\left[R_{0k}^3(\tau N_\mathrm{h})\right]=\frac{1}{L^3}\sum_{i=0}^{L-1}\mathrm{E}\left[\delta_\mathrm{K}\left(c_i^{(0)}-c_{[i-\tau]_L}^{(k)}\right)\right]$$
$$+\frac{3}{L^3}\sum_{\substack{i=0\\ i\neq j}}^{L-1}\sum_{j=0}^{L-1}\mathrm{E}\left[\delta_\mathrm{K}^2\left(c_i^{(0)}-c_{[i-\tau]_L}^{(k)}\right)\right]$$
$$\cdot\,\mathrm{E}\left[\delta_\mathrm{K}\left(c_j^{(0)}-c_{[j-\tau]_L}^{(k)}\right)\right]$$
$$+\frac{1}{L^3}\sum_{\substack{i=0\\ i\neq j,j\neq i',i'\neq i}}^{L-1}\sum_{j=0}^{L-1}\sum_{i'=0}^{L-1}\mathrm{E}\left[\delta_\mathrm{K}\left(c_i^{(0)}-c_{[i-\tau]_L}^{(k)}\right)\right]$$
$$\cdot\,\mathrm{E}\left[\delta_\mathrm{K}\left(c_j^{(0)}-c_{[j-\tau]_L}^{(k)}\right)\right]\mathrm{E}\left[\delta_\mathrm{K}\left(c_{i'}^{(0)}-c_{[i'-\tau]_L}^{(k)}\right)\right]$$
$$=\frac{1}{L^2}\left[\frac{1}{N_\mathrm{h}}+\frac{3(L-1)}{N_\mathrm{h}^2}+\frac{L(L-1)}{N_\mathrm{h}^3}\right]. \quad (26)$$

Taking a similar approach, the 4^{th} order moment is derived as

$$\mathrm{E}\left[R_{0k}^4(\tau N_\mathrm{h})\right]$$
$$=\frac{1}{L^4}\sum_{i=0}^{L-1}\sum_{j=0}^{L-1}\sum_{i'=0}^{L-1}\sum_{j'=0}^{L-1}\mathrm{E}\left[\delta_\mathrm{K}\left(c_i^{(0)}-c_{[i-\tau]_L}^{(k)}\right)\right.$$
$$\cdot\,\delta_\mathrm{K}\left(c_j^{(0)}-c_{[j-\tau]_L}^{(k)}\right)\cdot\delta_\mathrm{K}\left(c_{i'}^{(0)}-c_{[i'-\tau]_L}^{(k)}\right)$$
$$\left.\cdot\,\delta_\mathrm{K}\left(c_{j'}^{(0)}-c_{[j'-\tau]_L}^{(k)}\right)\right]$$
$$=\frac{1}{L^3}\left[\frac{1}{N_\mathrm{h}}+\frac{7(L-1)}{N_\mathrm{h}^2}+\frac{6L(L-1)}{N_\mathrm{h}^3}+\frac{LP_3}{N_\mathrm{h}^4}\right]. \quad (27)$$

B. DS-MA

Since all random parameters appearing in (10) are independent, the mean of $R_{0k}(\rho)$ is obtained as

$$\mathrm{E}\left[R_{0k}(\rho)\right]=\frac{1}{L}\sum_{j=0}^{L-1}\mathrm{E}\left[b_j^{(0)}\right]\mathrm{E}\left[b_{[j-\tau]_L}^{(k)}\right]\mathrm{E}\left[\delta_\mathrm{K}(\phi)\right]. \quad (28)$$

The n^{th} order moment of $b_j^{(k)}$ is equal to 1 if n is even and equal to 0 otherwise. Thus

$$\mathrm{E}\left[R_{0k}(\rho)\right]=0. \quad (29)$$

The 2^{nd} order moment is represented by

$$\mathrm{E}\left[R_{0k}^2(\rho)\right]=\frac{1}{L^2}\sum_{i=0}^{L-1}\sum_{j=0}^{L-1}\mathrm{E}\left[b_i^{(0)}b_{[i-\tau]_L}^{(k)}b_j^{(0)}b_{[j-\tau]_L}^{(k)}\right]$$
$$\cdot\,\mathrm{E}\left[\delta_\mathrm{K}^2(\phi)\right]. \quad (30)$$

Breaking the sum in (30) into two parts, it reduces to

$$\mathrm{E}\left[R_{0k}^2(\rho)\right]=\frac{1}{L^2N_\mathrm{h}}\sum_{i=0}^{L-1}\mathrm{E}\left[\left(b_i^{(0)}\right)^2\right]\mathrm{E}\left[\left(b_{[i-\tau]_L}^{(k)}\right)^2\right]$$
$$+\frac{1}{L^2N_\mathrm{h}}\sum_{\substack{i=0\\ i\neq j}}^{L-1}\sum_{j=0}^{L-1}\mathrm{E}\left[b_i^{(0)}\right]\mathrm{E}\left[b_{[i-\tau]_L}^{(k)}\right]\mathrm{E}\left[b_j^{(0)}\right]\mathrm{E}\left[b_{[j-\tau]_L}^{(k)}\right]$$
$$=\frac{1}{LN_\mathrm{h}}. \quad (31)$$

The 3^{rd} order moment is represented by

www.dbpia.co.kr

$$\begin{aligned}
&\mathrm{E}\left[R_{0k}^3(\rho)\right] \\
&= \frac{1}{L^3}\sum_{i=0}^{L-1}\sum_{j=0}^{L-1}\sum_{i'=0}^{L-1}\mathrm{E}\left[b_i^{(0)}b_{[i-\tau]_L}^{(k)}b_j^{(0)}b_{[j-\tau]_L}^{(k)}\right. \\
&\qquad \left. b_{i'}^{(0)}b_{[i'-\tau]_L}^{(k)}\right]\mathrm{E}\left[\delta_{\mathrm{K}}^3(\phi)\right] \\
&= \frac{1}{L^3 N_{\mathrm{h}}}\sum_{i=0}^{L-1}\mathrm{E}\left[\left(b_i^{(0)}\right)^3\right]\mathrm{E}\left[\left(b_{[i-\tau]_L}^{(k)}\right)^3\right] \\
&\quad + \frac{3}{L^3 N_{\mathrm{h}}}\sum_{\substack{i=0\\ i\neq j}}^{L-1}\sum_{j=0}^{L-1}\mathrm{E}\left[\left(b_i^{(0)}\right)^2\right]\mathrm{E}\left[\left(b_{[i-\tau]_L}^{(k)}\right)^2\right] \\
&\qquad \cdot \mathrm{E}\left[b_j^{(0)}\right]\mathrm{E}\left[b_{[j-\tau]_L^{(k)}}\right] \\
&\quad + \frac{1}{L^3 N_{\mathrm{h}}}\sum_{\substack{i=0\\ i\neq j, j\neq i', i'\neq i}}^{L-1}\sum_{j=0}^{L-1}\sum_{i'=0}^{L-1}\mathrm{E}\left[b_i^{(0)}\right]\mathrm{E}\left[b_{[i-\tau]_L^{(k)}}\right] \\
&\quad \cdot \mathrm{E}\left[b_j^{(0)}\right]\mathrm{E}\left[b_{[j-\tau]_L^{(k)}}\right]\mathrm{E}\left[b_{i'}^{(0)}\right]\mathrm{E}\left[b_{[i'-\tau]_L^{(k)}}\right].
\end{aligned} \tag{32}$$

Since every product term in the above equation contains the odd order moment of $b_j^{(k)}$, it reduces to

$$\mathrm{E}\left[R_{0k}^3(\rho)\right] = 0. \tag{33}$$

Now, the 4^{th} order moment can be expressed as

$$\begin{aligned}
&\mathrm{E}\left[R_{0k}^4(\tau N_{\mathrm{h}})\right] \\
&= \frac{1}{L^4}\sum_{i=0}^{L-1}\sum_{j=0}^{L-1}\sum_{i'=0}^{L-1}\sum_{j'=0}^{L-1}\mathrm{E}\left[b_i^{(0)}b_{[i-\tau]_L^{(k)}}b_j^{(0)}b_{[j-\tau]_L^{(k)}}\right. \\
&\left. \cdot\, b_{i'}^{(0)}b_{[i'-\tau]_L^{(k)}}b_{j'}^{(0)}b_{[j'-\tau]_L^{(k)}}\right]\mathrm{E}\left[\delta_{\mathrm{K}}^4(\phi)\right],
\end{aligned} \tag{34}$$

and is calculated by

$$\mathrm{E}\left[R_{0k}^4(\tau N_{\mathrm{h}})\right] = \frac{3L-2}{L^3 N_{\mathrm{h}}}. \tag{35}$$

2. Moments of MUI term for a single-path scenario

The moments of a_k appearing in the derivations in the following sections are calculated by

$$\mathrm{E}\left[a_k\right] = \frac{2\sqrt{G}}{d+d_0}, \tag{36}$$

$$\mathrm{E}\left[a_k^2\right] = \frac{2G}{d^2-d_0^2}\ln\frac{\mathrm{d}}{\mathrm{d}_0}, \tag{37}$$

$$\mathrm{E}\left[a_k^3\right] = \frac{2G\sqrt{G}}{dd_0(d+d_0)}, \tag{38}$$

$$\mathrm{E}\left[a_k^4\right] = \left(\frac{G}{dd_0}\right)^2. \tag{39}$$

A. TH-MA

For the TH case, assuming (7) as in section Ⅱ-1, I is approximated by

$$I \simeq \sum_{k=1}^{N_{\mathrm{u}}} a_k R_{0k}(\tau_k N_{\mathrm{h}}). \tag{40}$$

Since a_k and R_{0k} are independent, the expectation of I is calculated by

$$\begin{aligned}
\mathrm{E}[I] &\simeq \sum_{k=1}^{N_{\mathrm{u}}}\mathrm{E}\left[a_k\right]\mathrm{E}\left[R_{0k}(\tau_k N_{\mathrm{h}})\right] \\
&= N_{\mathrm{u}}\mathrm{E}\left[a_k\right]\mathrm{E}\left[R_{0k}(\tau_k N_{\mathrm{h}})\right].
\end{aligned} \tag{41}$$

Substituting (21) and (36) into (41), $\mathrm{E}[I]$ is obtained as

$$\mathrm{E}[I] \simeq \frac{N_{\mathrm{u}}}{N_{\mathrm{h}}}\left(\frac{2\sqrt{G}}{d+d_0}\right). \tag{42}$$

The 2^{nd} order moment can be approximated by

$$\begin{aligned}
\mathrm{E}\left[I^2\right] &\simeq \sum_{k=1}^{N_{\mathrm{u}}}\sum_{l=1}^{N_{\mathrm{u}}}\mathrm{E}\left[a_k a_l R_{0k}(\tau_k N_{\mathrm{h}})R_{0l}(\tau_l N_{\mathrm{h}})\right] \\
&= \sum_{k=1}^{N_{\mathrm{u}}}\mathrm{E}\left[a_k^2\right]\mathrm{E}\left[R_{0k}^2(\tau_k N_{\mathrm{h}})\right] \\
&\quad + \sum_{\substack{k=1\\ k\neq l}}^{N_{\mathrm{u}}}\sum_{l=1}^{N_{\mathrm{u}}}\mathrm{E}\left[a_k\right]\mathrm{E}\left[a_l\right]\mathrm{E}\left[R_{0k}(\tau_k N_{\mathrm{h}})\right] \\
&\quad \cdot \mathrm{E}\left[R_{0l}(\tau_l N_{\mathrm{h}})\right].
\end{aligned} \tag{43}$$

Because of independence of parameters, this reduces to

$$\mathrm{E}\left[I^2\right] \simeq N_{\mathrm{u}}\mathrm{E}\left[a_k^2\right]\mathrm{E}\left[R_{0k}^2(\tau_k N_{\mathrm{h}})\right] \tag{44}$$

The 3^{rd} order moment can expressed as

www.dbpia.co.kr

$$\mathrm{E}[I^3] \simeq \sum_{k=1}^{N_u}\sum_{l=1}^{N_u}\sum_{k'=1}^{N_u}\mathrm{E}[a_k a_l a_{k'}] + N_u(N_u-1)\left[\mathrm{E}[a_k]\right]^2\left[\mathrm{E}\left[R_{0k}(\tau_k N_h)\right]\right]^2. \quad (45)$$

Breaking the sum in (45) into three parts, it is calculated by

$$\mathrm{E}[I^3] \simeq \sum_{k=1}^{N_u}\mathrm{E}[a_k^3]\mathrm{E}\left[R_{0k}^3(\tau_k N_h)\right] + 3\sum_{\substack{k=1\\k\neq l}}^{N_u}\sum_{l=1}^{N_u}\mathrm{E}[a_k^2]\mathrm{E}[a_l] \cdot \mathrm{E}\left[R_{0k}^2(\tau_k N_h)\right]\mathrm{E}\left[R_{0l}(\tau_k N_h)\right]$$

$$+ \sum_{\substack{k=1\\k\neq l,l\neq k',k'\neq k}}^{N_u}\sum_{l=1}^{N_u}\sum_{k'=1}^{N_u}\mathrm{E}[a_k]\mathrm{E}[a_l]\mathrm{E}[a_{k'}] \cdot \mathrm{E}\left[R_{0k}(\tau_k N_h)\right]\mathrm{E}\left[R_{0l}(\tau_l N_h)\right]\mathrm{E}\left[R_{0k'}(\tau_{k'} N_h)\right]$$

$$= N_u\mathrm{E}[a_k^3]\mathrm{E}\left[R_{0k}^3(\tau_k N_h)\right] + {}_{N_u}P_3\left[\mathrm{E}[a_k]\right]^3\left[\mathrm{E}\left[R_{0k}(\tau_k N_h)\right]\right]^3 + 3N_u(N_u-1)\mathrm{E}[a_k^2]\mathrm{E}[a_k] \cdot \mathrm{E}\left[R_{0k}^2(\tau_k N_h)\right]\mathrm{E}\left[R_{0k}(\tau_k N_h)\right]. \quad (46)$$

Using a similar method, the 4^{th} order moment is derived as

$$\mathrm{E}[I^4] \simeq N_u\mathrm{E}[a_k^4]\mathrm{E}\left[R_{0k}^4(\tau_k N_h)\right] + 3N_u(N_u-1)\left[\mathrm{E}[a_k^2]\right]^2\left[\mathrm{E}\left[R_{0k}^2(\tau_k N_h)\right]\right]^2 + 4N_u(N_u-1)\mathrm{E}[a_k^3]\mathrm{E}[a_k] \cdot \mathrm{E}\left[R_{0k}^3(\tau_k N_h)\right]\mathrm{E}\left[R_{0k}(\tau_k N_h)\right] + 6\,{}_{N_u}P_3\mathrm{E}[a_k^2]\left[\mathrm{E}[a_k]\right]^2\mathrm{E}\left[R_{0k}^2(\tau_k N_h)\right] \cdot \left[\mathrm{E}\left[R_{0k}(\tau_k N_h)\right]\right]^2 + {}_{N_u}P_4\mathrm{E}[a_k^4]\mathrm{E}\left[R_{0k}^4(\tau_k N_h)\right]. \quad (47)$$

The moments of a^k appearing in (44), (46), and (47) are given by (36)-(39). And the moments of $R_{0k}(\tau_k N_h)$ are given by (21),(24),(26), and (27).

B. DS-MA

For the DS case, the mean of I is given by

$$\mathrm{E}[I] = \sum_{k=1}^{N_u}\mathrm{E}[a_k]\mathrm{E}\left[R_{0k}(\rho_k)\right] = 0, \quad (48)$$

and the 2^{nd} order moment is obtained as

$$\mathrm{E}[I^2] = \sum_{k=1}^{N_u}\sum_{l=1}^{N_u}\mathrm{E}[a_k a_l]\mathrm{E}\left[R_{0k}(\rho_k)R_{0l}(\rho_l)\right] = \sum_{k=1}^{N_u}\mathrm{E}[a_k^2]\mathrm{E}\left[R_{0k}^2(\rho_k)\right] + \sum_{\substack{k=1\\k\neq l}}^{N_u}\sum_{l=1}^{N_u}\mathrm{E}[a_k]\mathrm{E}[a_l]\mathrm{E}\left[R_{0k}(\rho_k)\right]\mathrm{E}\left[R_{0l}(\rho_l)\right]$$

$$= N_u\mathrm{E}[a_k^2]\mathrm{E}\left[R_{0k}^2(\rho_k)\right]. \quad (49)$$

Substituting (31) and (37) into (49),

$$\mathrm{E}[I^2] = \left(\frac{N_u}{LN_h}\right)\left(\frac{2G}{d^2-d_0^2}\right)\ln\frac{d}{d_0}. \quad (50)$$

Now, expressing $\mathrm{E}[I^3]$ in a similar form as in (46),

$$\mathrm{E}[I^3] = \sum_{k=1}^{N_u}\mathrm{E}[a_k^3]\mathrm{E}\left[R_{0k}^3(\tau_k N_h)\right] + 3\sum_{\substack{k=1\\k\neq l}}^{N_u}\sum_{l=1}^{N_u}\mathrm{E}[a_k^2]\mathrm{E}[a_l] \cdot \mathrm{E}\left[R_{0k}^2(\tau_k N_h)\right]\mathrm{E}\left[R_{0l}(\tau_k N_h)\right]$$

$$+ \sum_{\substack{k=1\\k\neq l,l\neq k',k'\neq k}}^{N_u}\sum_{l=1}^{N_u}\sum_{k'=1}^{N_u}\mathrm{E}[a_k]\mathrm{E}[a_l]\mathrm{E}[a_{k'}] \cdot \mathrm{E}\left[R_{0k}(\tau_k N_h)\right]\mathrm{E}\left[R_{0l}(\tau_l N_h)\right]\mathrm{E}\left[R_{0k'}(\tau_{k'} N_h)\right]. \quad (51)$$

Since all product terms in (51) contain the odd order moment of $\mathrm{E}[I^3]$, it reduces to

$$\mathrm{E}[I^3] = 0. \quad (52)$$

www.dbpia.co.kr

Using a similar method, the $\mathrm{E}\left[I^4\right]$ order moment can be derived as

$$\mathrm{E}\left[I^4\right]=N_{\mathrm{u}}\mathrm{E}\left[a_k^4\right]\mathrm{E}\left[R_{0k}^4(\rho_k)\right] +3N_{\mathrm{u}}(N_{\mathrm{u}}-1)\left[\mathrm{E}\left[a_k^2\right]\right]^2\left[\mathrm{E}\left[R_{0k}^2(\rho_k)\right]\right]^2, \quad (53)$$

where $\mathrm{E}\left[R_{0k}^2(\rho_k)\right]$, $\mathrm{E}\left[R_{0k}^4(\rho_k)\right]$, $\mathrm{E}\left[a_k^2\right]$, and $\mathrm{E}\left[a_k^4\right]$ are given by (31), (35), (37), and (39), respectively.

References

[1] C.-P. Yoon and C.-G. Hwang, "Efficient indoor positioning systems for indoor location-based service provider," *J. KIICE* vol. 19, no. 6, pp. 1368-1373, 2015.

[2] D.-Y. Choi, et al., "Design and implementation of tapered slot antenna for ship's indoor location-aware system," *J. KICS*, vol. 39, no. 12, pp. 1307-1313, 2014.

[3] J.-W. Kim, J.-H. Park, and S. R. Lee, "Collision avoidance method for coexistence between relay-based multi-hop UWB system," *J. KICS*, vol. 39, no. 8, pp. 688-695, 2014.

[4] J.-Y. Lee and S. Yoo, "Performance of UWB ranging in multipath and multiuser environments," *J. KICS*, vol. 30, no. 12C, pp. 1125-1132, 2006.

[5] J.-Y. Lee and R. A. Scholtz, "Ranging in a dense multipath environment using an UWB radio link," *IEEE J. Sel. Areas in Commun.*, vol. 20, no. 9, pp. 1677-1683, 2002.

[6] P. H. Westfall, "Kurtosis as peakedness, 1905 – 2014. RIP," *The Am. Statistician*, vol. 68, no. 3, pp. 191-195, 2014.

[7] Wikipedia, "Kurtosis — wikipedia, the free encyclopedia," http://en.wikipedia.org/wiki/Kurtosis, 2016. [Online; accessed 02 Jun. 2016]

[8] R. A. Scholtz, P. V. Kumar, and C. J. Corrada-Bravo, "Signal design for ultra-wideband radio," in *Proc. Sequences and their Applications*, pp. 72-87, Springer, 2002.

[9] C. Corrada-Bravo, R. Scholtz, and P. Kumar, "Good correlation and approximately flat PSD level," in *Proc. Ultra Wideband Conf.*, Sept. 1999.

[10] T. Erseghe, "Time-hopping patterns derived from permutation sequences for ultra-wide-band impulse-radio applications," in *Proc. 6th WSEAS Int. Conf. Commun.*, vol. 1, pp. 109-115, Citeseer, 2002.

[11] I. Guvenc and H. Arslan, "Design and performance analysis of TH sequences for UWB-IR systems," in *Proc. IEEE Wireless Commun. and Netw. Conf.*, vol. 2, pp. 914-919 vol. 2, Mar. 2004.

[12] Z. Zhang, F. Zeng, and L. Ge, "Time-hopping sequences construction with few-hit zone for quasi-synchronous THSS-UWB systems," in *Proc. 2005 IEEE 61st Veh. Technol. Conf.*, vol. 3, pp. 1998-2002, vol. 3, May 2005.

[13] M. S. Iacobucci and M. G. D. Benedetto, "Time hopping codes in impulse radio multiple access communication systems," in *Proc. Int. Workshop on 3G Infrastructure and Services*, pp. 171-175, Athens, Greece, 2001.

[14] C. Muller, S. Zeisberg, H. Seidel, and A. Finger, "Spreading properties of time hopping codes in ultra wideband systems," in *Proc. 2002 IEEE 7th Int. Symp. Spread Spectrum Techniques and Appl.*, vol. 1, pp. 64-67 vol. 1, 2002.

[15] L. Piazzo and J. Romme, "Spectrum control by means of the TH code in UWB systems," in *Proc. VTC 2003-Spring*, vol. 3, pp. 1649-1653 vol.3, Apr. 2003.

[16] H. Shao and N. C. Beaulieu, "Direct sequence and time-hopping sequence designs for narrowband interference mitigation in impulse radio UWB systems," *IEEE Trans. Commun.*, vol. 59, pp. 1957-1965, Jul. 2011.

[17] J. Bellorado, S. S. Ghassenzadeh, A. Kavcic, B. Tarokh, and V. Tarokh, "Time-hopping sequence design for narrowband interference suppression," in *Proc. 2004 IEEE 60th VTC*, vol. 6, pp. 3925-3929, Sept. 2004.

[18] R. A. Scholtz, "Multiple access with time-hopping impulse modulation," in *Proc. IEEE MILCOM '93*, vol. 2, pp. 447-450, vol. 2, Oct. 1993.

www.dbpia.co.kr

[19] M. Hamalainen, J. Iinatti, V. Hovinen, and M. Latva-aho, “In-band interference of three kinds of UWB signals in GPS L1 band and GSM900 uplink band,” in *Proc. 12th IEEE Int. Symp. Pers., Indoor and Mob. Radio Commun.*, vol. 1, pp. D‐76‐D‐80, vol. 1, Sept. 2001.

[20] J.-Y. Lee, “UWB channel modeling in roadway and indoor parking environments,” *IEEE Trans. Veh. Technol.*, vol. 59, pp. 3171-3180, Sept. 2010.

이 준 용 (Joon-Yong Lee)

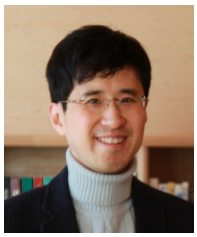

1993년 2월 : 홍익대학교 전자공학과 학사 졸업

1997년 5월 : University of Southern California 전자공학과 석사 졸업

2002년 5월 : University of Southern California 전자공학과 박사 졸업

2002년 9월~현재 : 한동대학교 전산전자공학부 교수

<관심분야> UWB 위치추적시스템, UWB 레이더 센서네트워크, UWB 채널 모델링

www.dbpia.co.kr